



UNIVERSITY OF LEEDS

This is a repository copy of *Decoupling seasonal fluctuations in fluvial discharge from the tidal signature in ancient deltaic deposits: an example from the Neuquén Basin, Argentina*.

White Rose Research Online URL for this paper:  
<http://eprints.whiterose.ac.uk/88814/>

Version: Accepted Version

---

**Article:**

Gugliotta, M, Kurcinka, CE, Dalrymple, RW et al. (2 more authors) (2016) Decoupling seasonal fluctuations in fluvial discharge from the tidal signature in ancient deltaic deposits: an example from the Neuquén Basin, Argentina. *Journal of the Geological Society*, 173 (1). pp. 94-107. ISSN 0016-7649

<https://doi.org/10.1144/jgs2015-030>

---

**Reuse**

Unless indicated otherwise, fulltext items are protected by copyright with all rights reserved. The copyright exception in section 29 of the Copyright, Designs and Patents Act 1988 allows the making of a single copy solely for the purpose of non-commercial research or private study within the limits of fair dealing. The publisher or other rights-holder may allow further reproduction and re-use of this version - refer to the White Rose Research Online record for this item. Where records identify the publisher as the copyright holder, users can verify any specific terms of use on the publisher's website.

**Takedown**

If you consider content in White Rose Research Online to be in breach of UK law, please notify us by emailing [eprints@whiterose.ac.uk](mailto:eprints@whiterose.ac.uk) including the URL of the record and the reason for the withdrawal request.



[eprints@whiterose.ac.uk](mailto:eprints@whiterose.ac.uk)  
<https://eprints.whiterose.ac.uk/>

1 **Title: Decoupling seasonal fluctuations in fluvial discharge from the tidal signature in**  
2 **ancient deltaic deposits: an example from the Neuquén Basin, Argentina**

3

4 **Running title: fluvial and tidal signals in sedimentation**

5

6 Marcello Gugliotta <sup>1\*</sup>, Colleen E. Kurcinka <sup>2</sup>, Robert W. Dalrymple <sup>2</sup>, Stephen S. Flint <sup>1</sup>,

7 David M. Hodgson <sup>3</sup>

8

9 <sup>1</sup> Stratigraphy Group, School of Earth, Atmospheric and Environmental Sciences, University  
10 of Manchester, UK

11 <sup>2</sup> Department of Geological Sciences and Geological Engineering, Queen's University,  
12 Kingston, Ontario, Canada

13 <sup>3</sup> Stratigraphy Group, School of Earth and Environment, University of Leeds, UK

14 \* marcello.gugliotta@manchester.ac.uk

15

16 **Keywords:**

17 **River discharge, seasonality, heterolithic, IHS, tidalite**

18 **Abstract**

19 Fluvial discharge fluctuations are a fundamental characteristic of almost all modern rivers  
20 and can produce distinctive deposits that are rarely described from ancient fluvial or mixed-  
21 energy successions. Large-scale outcrops from the Middle Jurassic Lajas Formation  
22 (Argentina) expose a well-constrained stratigraphic succession of marginal-marine deposits  
23 with a strong fluvial influence and well-known tidal indicators. The studied deposits show  
24 decimetre-scale interbedding of coarser- and finer-grained facies with mixed fluvial and tidal  
25 affinities. The alternation of these two types of beds forms non-cyclic successions that are  
26 interpreted to be the result of seasonal variation in river discharge, rather than regular and  
27 predictable changes in current velocity caused by tides. Seasonal bedding is present in bar  
28 deposits that form within or at the mouth of minor and major channels. Seasonal bedding is  
29 not preserved in channel thalweg deposits, where river flood processes were too powerful, or  
30 in floodplain, muddy interdistributary bay, prodelta and transgressive deposits, where the  
31 river signal was weak and sporadic. The identification of sedimentary facies characteristic of  
32 seasonal river discharge variations is important for accurate interpretation of ancient deltaic  
33 process regime.

34

35

36 Heterolithic deposits consisting of interlaminated and/or interbedded sandstone and mudstone  
37 include inclined heterolithic strata (IHS), flaser, wavy and lenticular bedding, and fluid mud-  
38 sand couplets (Reineck and Wunderlich 1968; Thomas et al. 1987; Ichnas and Dalrymple  
39 2009; MacKay and Dalrymple 2011). These features are commonly identified in tidal  
40 depositional systems (Nio and Yang 1991; Dalrymple and Choi 2007; Geel and Donselaar  
41 2007; Choi 2010; Dalrymple 2010; Davis 2012) and are often used to infer a tidal origin of  
42 ancient deposits. However, heterolithic deposits can also form in purely fluvial or mixed-  
43 energy settings due to temporal variations in river discharge at a seasonal or shorter time  
44 scale (Thomas et al. 1987) but in such settings they lack the ordered cyclicality of layer  
45 thickness and grain size that characterizes tidal sedimentation (Archer 1995; Kvale et al.  
46 1995; Kvale 2012). River discharge fluctuations are a fundamental characteristic of almost all  
47 modern rivers (Milliman and Farnsworth 2011) and can also coexist with tidal processes in  
48 the deposits that accumulate in the lower reaches of rivers (e.g. Fraser River delta, Canada;  
49 Sisulak and Dashtgard 2012; Johnson and Dashtgard 2014), making it difficult to assess the  
50 relative importance of tidal and river currents.

51 In ancient successions tidal sedimentary structures (e.g. bundling, drapes, rhythmic  
52 lamination, bidirectional palaeocurrents, etc.), have received considerable attention (e.g.  
53 Visser 1980; Allen 1981; De Boer et al. 1989; Dalrymple et al. 1992; Willis 2005; Dalrymple  
54 and Choi 2007; Dalrymple et al. 2012; Plink-Björklund 2012; Legler et al. 2013) whereas  
55 facies associated with the seasonal variation of river discharge have received comparatively  
56 little emphasis (Bridge 2003; Rebata et al. 2006). The paucity of examples that describe river-  
57 generated seasonal bedding in the rock record may be hampered by the lack of a well-defined  
58 facies model. Discriminating between tidal and fluvial processes as the main control on  
59 deposition in the fluvial to marine transition zone (Dalrymple and Choi 2007) is crucial for

60 improving and refining depositional models at the facies scale (Martinius et al. 2005; Nordahl  
61 et al. 2006), and for predicting the larger-scale geometry of sedimentary bodies (Reynolds  
62 1999). Moreover, the recognition of fluvially generated seasonal deposits will improve  
63 palaeoclimatic and palaeogeographic reconstructions, particularly when other approaches  
64 (e.g. palaeobotanical, palaeontological) are not available or are non-diagnostic. The aims of  
65 this paper are: i) to establish recognition criteria to help distinguish between seasonal-  
66 discharge and tidal-process signals in the rock record and ii) to discuss how the tidal and  
67 seasonal signals are recorded in different facies, in order to help refine palaeoenvironmental  
68 reconstructions.

69 Large-scale outcrops from the Middle Jurassic Lajas Fm. (Argentina) provide a well-  
70 constrained succession of marginal-marine deposits (Zavala 1996a, b; Brandsaeter et al.  
71 2005; McIlroy et al. 2005; Kurcinka 2014; Gugliotta et al. 2015). These deposits contain  
72 well-known tidal indicators, and a strong fluvial influence, which are recorded in both  
73 heterolithic and sandstone-dominated deposits that are described in detail herein. Tide-  
74 dominated dunes and bars described in Zavala (1996a, b) and Martinus and Van den Berg  
75 (2011) are present in specific stratigraphic intervals but are not the focus of this paper.

76

### 77 **Discharge fluctuations in modern rivers**

78 Of the 1534 present-day rivers in the database of Milliman and Farnsworth (2011), almost  
79 95% show variations in discharge through the year (Fig. 1). In most of the rivers in low- and  
80 mid-latitudes, discharge fluctuations reflect a direct response to precipitation, which may be  
81 driven by the monsoon (Purnachandra Rao et al. 2011), whereas rivers in high latitude and  
82 high elevation areas, exhibit discharge variations that are affected by the melting of snow and  
83 ice (Milliman and Farnsworth 2011; La Croix and Dashtgard 2014).

84 In systems with large catchment areas and relatively high runoff rates, the effects of  
85 individual rainfall events are dampened and only the longer-term, annual variation in runoff  
86 is recorded in the deposits (Allen and Chambers 1998). In systems with small catchment  
87 areas and/or relatively arid runoff conditions, flow generally responds to individual rainfall  
88 events and is not as obviously tied to the general climatic conditions (Gonzalez-Hidalgo et al.  
89 2010; Gonzalez-Hidalgo et al. 2013), in which case there might be more than one river flood  
90 in a single year. In large rivers, the flood stage can last for weeks to months, whereas in small  
91 rivers the flood may be over in a few hours. The influence of individual precipitation events  
92 increases with a reduction of catchment size because the impact of peak events in small  
93 drainage basins reflects the erosive power of flash floods and the inability of small basins to  
94 absorb local precipitation (Gonzalez-Hidalgo et al. 2010; Gonzalez-Hidalgo et al. 2013). In  
95 flashy rivers, the discharge rises quickly, often by two to four orders of magnitude in a single  
96 day (Fielding and Alexander 1996). In perennial rivers, by contrast, the discharge rises from  
97 low flow to peak flood discharge more slowly and the difference between the two is  
98 commonly small (i.e. peak discharge is commonly only one order of magnitude larger than  
99 low flow). For example, in the Fraser River, during low flow the discharge rate is ca  $1000 \text{ m}^3$   
100  $\text{sec}^{-1}$ , and increases up to  $15200 \text{ m}^3 \text{ sec}^{-1}$  during high flow (La Croix and Dashtgard 2014),  
101 while in the Mississippi River, the minimum mean monthly water discharge is about  $2900 \text{ m}^3$   
102  $\text{sec}^{-1}$ , whereas maximum mean monthly water discharge reaches  $52000\text{--}55000 \text{ m}^3 \text{ sec}^{-1}$   
103 (Mikhailov and Mikhailova 2010).

104 Recently, particular attention has been given to the interaction of seasonal discharge  
105 fluctuations and tidal processes in modern, fluvial-tidal, mixed-energy settings (van Maren  
106 and Hoekstra 2004; Dark and Allen 2005; van den Berg et al. 2007; Sisulak and Dashtgard  
107 2012; Johnson and Dashtgard 2014). During the period of seasonal high river discharge, the  
108 effects of fluvial processes are extended seaward, reducing tidal and salinity effects and

109 pushing the tidal and salt wedge limits seaward (Allen et al. 1980; Dalrymple and Choi 2007;  
110 van den Berg et al. 2007; Kravtsova et al. 2009; Dalrymple et al. 2012; Dashtgard et al.  
111 2012), which also has implications for the location of the turbidity maximum and the  
112 distribution of mud in the system (Purnachandra Rao et al. 2011; La Croix and Dashtgard  
113 2014).

114

### 115 **Geological background**

116 The Neuquén Basin is an important hydrocarbon-producing sedimentary basin (Zambrano  
117 and Yrigoyen 1995) located in central-western Argentina and extending into east-central  
118 Chile, between 32° S and 40° S latitude (Fig. 2A). It covers more than 137,000 km<sup>2</sup> (Urien  
119 and Zambrano 1994) extending up to 700 km in a north-south direction and up to 400 km  
120 from west to east. The basin originated as a volcanic rift in the Triassic and evolved into a  
121 post-rift back-arc basin during the Jurassic. It is bounded on its north-eastern, eastern and  
122 southern margins by wide cratonic areas, which were the main source areas for the basin-fill  
123 sediment during the Jurassic (Uliana and Legarreta 1993), and by a magmatic arc on the  
124 active margin of the Gondwanan–South American Plate to the west (Howell et al. 2005). The  
125 Lajas Formation was deposited diachronously as a series of N and NW prograding wedges  
126 during the late Middle Jurassic (Fig. 3) and comprises more than 500 m of sandstone-,  
127 heterolithic- and mudstone-dominated deposits that accumulated in a variety of marginal-  
128 marine settings. The deltaic nature of most of the Lajas Fm. has been recognized in several  
129 studies (Spalletti 1995; Zavala 1996a, b; McIlroy et al. 2005) and for the last two decades has  
130 been interpreted as a tide-dominated system (McIlroy et al. 1999; Brandsaeter et al. 2005;  
131 McIlroy et al. 2005; Morgans-Bell and McIlroy 2005). More recently, however, the degree of  
132 tidal influence preserved in the delta plain to delta front deposits of the Lajas Fm. has been  
133 questioned (Kurcinka 2014; Gugliotta et al. 2015).

134 During the Middle Jurassic, South America was located in a similar orientation and latitude  
135 to the present-day configuration (Iglesia Llanos et al. 2006; Iglesia Llanos 2012) and was part  
136 of the west margin of the Gondwanan continent. The palaeoclimate of the study area has been  
137 interpreted by several palynological studies as warm and mainly arid, but with variable  
138 humidity (Quattrocchio et al. 2001; Martinez et al. 2002; Garcia et al. 2006; Stukins et al.  
139 2013).

140

#### 141 **Methods and dataset**

142 The stratigraphy of the Lajas Fm. has been investigated along 2 main cliff exposures near the  
143 village of Los Molles (Fig. 2B). Cliff-line A is SSW-NNE oriented and provides continuous  
144 exposure for about 8 km, whereas cliff-line B is oriented E-W and extends for approximately  
145 10 km. Both cliff-lines are oriented at an oblique angle to the regional palaeoflow, which is  
146 broadly toward the NW (Zavala and González 2001; McIlroy et al. 2005). Numerous canyon  
147 exposures provide three-dimensional constraint on the stratigraphic architecture at the small  
148 to intermediate scale. This paper describes deposits from intervals through the entire 500 m-  
149 thick Lajas Fm. in a proximal to distal sense (from purely fluvial channels to the prodelta)  
150 and across depositional strike (from distributary channel axes to the flanking interdistributary  
151 bay deposits). Data collection included detailed measured stratigraphic sections, integrated  
152 with annotated photopanel, in order to document the stratal architecture, correlation of the  
153 main stratigraphic surfaces, and lateral and vertical facies variations. Photopanel correlations  
154 were verified by physical tracing (walking out) of contacts. More than 70 GPS located  
155 sections were logged at 1:50 and 1:25 scale. Facies and facies associations were interpreted in  
156 terms of depositional processes and environments based on grain size, sorting, stratal  
157 geometries, sedimentary structures and the presence and character of body and trace fossils.

158

159 **Facies associations**

160 In this section, we describe the deposits and interpret the major depositional environments  
161 based on facies, process sedimentology and stratigraphic context. Detailed description of the  
162 nature of the interbedding is provided in the next section. Facies are grouped into eight facies  
163 associations (FA 1 to FA 8). Bioturbation intensity is generally low but highly variable, and  
164 is described in terms of Bioturbation Index (BI) from 0 to 6 (Taylor and Goldring 1993;  
165 MacEachern et al. 2010).

166

167 *FA 1: Fluvial and distributary channel deposits*

168 Description: FA 1 consists mainly of moderately to well-sorted sandstone, up to very coarse-  
169 grained, with sparse granules and subordinate heterolithic and mudstone deposits. Units of  
170 FA 1 are up to 12 m thick and laterally extensive for several hundred metres to over one  
171 kilometre. They are erosionally based, lenticular and show fining- and thinning-upward  
172 trends (Fig. 4A). FA 1 deposits are either structureless or show unidirectional, N or NW  
173 (seaward-directed), trough and planar-tabular cross-stratification, but also includes units of  
174 interbedded inclined coarser- and finer-grained sandstone and heterolithic beds (Fig. 4A, B,  
175 C). Beds are up to 0.4 m thick and laterally extensive for tens of metres. Depositional dip of  
176 the inclined master bedding is commonly perpendicular to the orientation of the cross-  
177 stratification. Some of the cross-stratification shows randomly-distributed carbonaceous  
178 drapes, but cyclical carbonaceous drapes are present in places. The cross-stratified facies is  
179 typically unidirectional and seaward-oriented and shows distribution of drapes composed of  
180 carbonaceous debris, commonly associated with plant debris and mica. Drapes are found in  
181 groups of 2-5 that are separated by a few millimetres to centimetres of sandstone whereas  
182 groups of drapes show spacing of several decimetres (Fig, 5A). This facies can show cyclical  
183 patterns in the distribution of drapes and height reached by the drapes on the foresets (Fig.

184 5B), as also described by Martinius and Gowland (2011). This facies lacks the features  
185 typical of the dominant current, slack water and subordinate tidal current, such as cyclically  
186 distributed reactivation surfaces, opposite directed ripples, and single and double mud drapes  
187 (Visser 1980). Pieces of silicified wood up to 1 m long are present and are typically oriented  
188 in the direction of the palaeoflow. Trace-fossil content is generally low (BI 0-1) and consists  
189 mainly of *Planolites*.

190

191 Interpretation: FA 1 is interpreted as fluvial and distributary channel deposits. The  
192 structureless and trough- and planar-tabular cross-stratified sandstones are interpreted as  
193 channel-axis deposits, whereas the inclined, interbedded coarser- and finer-grained  
194 sandstones indicate lateral accretion and are interpreted as bank-attached side bars and point  
195 bars. The interbedded finer- and coarser-grained beds are interpreted to reflect fluctuations in  
196 current speed as a result of changes in river discharge. The presence of unidirectional,  
197 seaward-oriented palaeocurrents in cross-stratification indicate fluvial dominance; minor tidal  
198 influence is indicated by the presence of cyclical carbonaceous drapes (Martinius and  
199 Gowland 2011), whereas the non-cyclical carbonaceous drapes are not considered to have  
200 been generated by tides, but instead to reflect non-periodic fluctuations of the river currents.  
201 The cyclically-distributed carbonaceous drapes are interpreted to reflect acceleration and  
202 deceleration (tidal modulation or tidal backwater effect) of fluvial currents, formed in the  
203 fluvial-dominated part of the fluvial to marine transition zone (Dalrymple and Choi 2007;  
204 Martinius and Gowland 2011; Dashtgard et al. 2012).

205

206 *FA 2: Floodplain and crevasse-splay deposits*

207 Description: FA 2 consists of poorly sorted, structureless or weakly laminated mudstones  
208 ranging from dark grey (with abundant detrital plant matter), to green, blue, purple and red

209 (scarce plant matter). This FA forms tabular units up to several tens of metres thick, laterally  
210 extensive for several kilometres, and intimately associated with FA 1. A minor facies within  
211 FA2 consists of tabular, structureless sandstone beds, a few tens of centimetres thick that  
212 form units up to 1 m thick and extend laterally for tens to hundreds of metres. Large pieces of  
213 silicified wood up to 8 m long are present along with root traces. The trace-fossil content  
214 consists of root traces that generally are abundant in mudstones (BI 6), but absent in the  
215 sandstone beds (BI 0).

216

217 Interpretation: The tabular, laterally extensive mudstone units of FA 2 are interpreted as  
218 largely subaerial floodplain deposits. The variations in colour and amount of organic matter  
219 are interpreted to reflect different states of oxidation, which are probably linked to the level  
220 of the water table and, in general, the distance from the coastline (Retallack 2008; Varela et  
221 al. 2012). The dark, organic-rich floodplain deposits may have formed in distal positions and  
222 under conditions of poor drainage, whereas the green-blue and purple-red deposits may  
223 represent relatively more proximal, inland positions with moderate to well-drained floodplain  
224 conditions. The lenticular and tabular sandstone units are interpreted as the deposits of  
225 crevasse splays.

226

### 227 *FA 3: Minor distributary channel deposits*

228 Description: FA 3 consists of erosionally based, lenticular, fining- and thinning-upward units  
229 up to 1.5 m thick that are laterally extensive for a few tens of metres (Fig. 4D). FA 3 usually  
230 erosionally overlies FA 2 and FA 4 deposits and is laterally associated with FA 1. FA 3 is  
231 commonly heterolithic with local high mudstone content. Sandstones range from very fine-  
232 grained to coarse-grained and are poorly to well sorted. These deposits can show dm-scale  
233 interbedding of inclined, thinning-upward, coarser- and finer-grained beds. Beds are

234 structureless or show unidirectional trough and planar-tabular cross-stratification and ripple  
235 cross-lamination or subordinate bidirectional ripples and non-cyclical rhythmmites with  
236 mudstone and carbonaceous drapes. Carbonaceous drapes can also show cyclical patterns.  
237 Palaeocurrents show a wide range of directions, but are mainly toward the N and NW; they  
238 are generally unidirectional within a single unit. Subordinate palaeocurrents are broadly  
239 toward the S (landward). Dipping of the inclined master bedding is commonly perpendicular  
240 to the cross-stratification. In some parts of FA 3, however, the coarser- and finer-grained  
241 couplets are not well-developed and structureless sandstones or flaser, wavy and lenticular  
242 bedding with rare bidirectional current ripples are present. Trace-fossil content is generally  
243 low (BI 0-1) and consists mainly of *Planolites* and *Dactyloidites*.

244

245 Interpretation: FA 3 is interpreted as minor distributary channel deposits, eroding into the  
246 subaerial delta plain (FA 2) and linked to the main distributive system (FA 1). FA 3 is distinct  
247 from FA 1 as the channels are considerably smaller (~1 m thick versus 4-12 m thick) and  
248 consist of more heterolithic deposits or less well-sorted, muddy sandstones. The alternating,  
249 inclined finer- and coarser-grained beds are interpreted as laterally accreting bars with a  
250 prevalence of unidirectional, seaward-oriented bedforms; sedimentation was, therefore,  
251 fluviially dominated. However, the presence of cyclic rhythmmites with mudstone drapes and  
252 bidirectional ripples suggests that the fluvial signal may be locally and temporally  
253 overprinted by tidal reworking. Carbonaceous drapes might result either from random  
254 fluctuations in the strength of the river current or tidal modulation of the fluvial current.

255

256 *FA 4: Crevasse mouth bar deposits*

257 Description: Typically, FA 4 consists of coarsening- and thickening-upward heterolithic  
258 units, up to 2 m thick (Fig. 6A), that are laterally extensive for tens to hundreds of metres. FA

259 4 gradually passes vertically and laterally into FA 7 and is incised by FA 1 and FA 3.  
260 Internally, units of FA 4 comprise alternations of medium-/coarse-grained and fine-grained  
261 beds that can be traced from only a few metres up to a few tens of metres. The beds are  
262 inclined and dip at up to 15-20 degrees, but commonly at lower angles (5-8 degrees). In the  
263 upper parts of FA 4, the coarser-grained beds are thicker and amalgamated, and the finer-  
264 grained intervening deposits may be missing such that the interbedding is not as clearly  
265 distinguishable as it is in the lower part of the unit (Fig. 6A). Coarser-grained beds are  
266 structureless or show unidirectional cross-stratification and ripple-cross-lamination. Finer-  
267 grained beds show internal mm-scale rhythmites with mudstone drapes and rare bidirectional  
268 ripples (Fig. 6B, C). The dips of the master bedding and cross-bedding show a wide range of  
269 directions, but both show a general prevalence toward the NW to NE (seaward-directed).  
270 The trace-fossil abundance is highly variable (BI 0-5).

271

272 Interpretation: FA 4 is interpreted as the deposits of mouth bars of crevasse delta systems.  
273 The common orientation of the inclined master bedding and cross-bedding indicate forward  
274 accretion. The alternating finer- and coarser- beds are interpreted to reflect fluctuations of  
275 river discharge, that together with the prevalence of unidirectional, seaward-directed  
276 palaeocurrents indicate river dominance. In the finer-grained beds, a tidal origin can be  
277 argued because of the presence of bidirectional ripples, mudstone drapes and a brackish water  
278 trace fossil assemblage. The poor sorting is attributed to the presence of high turbidity and  
279 entrainment of mud during deposition. The association with FA 1, FA 3 and FA 7 and the  
280 poor sorting suggest that FA 4 formed in interdistributary-bays of lower-delta-plain settings  
281 (Gugliotta et al. 2015).

282

283 *FA 5: Terminal distributary channel deposits*

284 Description: FA 5 consists of fine- to medium-grained, moderately to well-sorted, lenticular,  
285 erosionally-based sandstones up to 3 m thick that are laterally extensive up to a few tens of  
286 metres. FA 5 is usually structureless or trough-cross-stratified and is erosive into FA 6.  
287 Cross-stratification can show cyclically-distributed carbonaceous drapes. Palaeocurrents are  
288 commonly unidirectional to the N and NW (seaward-oriented), although rare S- (landward-)  
289 directed palaeocurrents were recorded. Trace-fossil abundance and biodiversity are generally  
290 low (BI 0-1), although rare examples show BI levels up to 5.

291

292 Interpretation: FA 5 is interpreted as terminal distributary channel deposits because of their  
293 relatively small size and intimate association with mouth bar deposits (FA 6). The  
294 predominantly unidirectional, seaward-oriented palaeocurrents suggest river dominance,  
295 consistent with the setting in which terminal distributary channels form (Olariu and  
296 Bhattacharya 2006). The rare landward-directed palaeocurrents and cyclically-distributed  
297 carbonaceous drapes suggest subordinate tidal influence at times.

298

#### 299 *FA 6: Mouth bar deposits*

300 Description: FA 6 consists of coarsening- and thickening-upward units (Fig. 7A), up to 12 m  
301 thick, that form bodies several kilometres in lateral extent. FA 6 gradually passes downward  
302 and laterally into FA 7 and is erosionally incised by FA 1 and FA 5. FA 6 is composed of  
303 decimetre-scale interbedded fine-/medium-grained and very fine-/fine-grained sandstone  
304 (Fig. 7B, C, D, E). Beds are up to 0.4 m thick, dip at up to 15 degrees and show internal  
305 unidirectional, trough and planar-tabular cross-bedding and ripple-cross lamination oriented  
306 toward the N and NW, with subordinate, bidirectional ripples and rhythmites with mudstone  
307 drapes. The inclination of master bedding and cross-bedding are both seaward-directed and  
308 parallel to each other. In the upper part of FA 6, the coarser-grained beds are thicker and

309 amalgamated (Fig. 7B), and the finer-grained intervening deposits may be missing. Trace-  
310 fossil abundance is highly variable (BI 0-6), but the diversity is generally low.

311

312 Interpretation: FA 6 is interpreted as mouth-bar deposits that formed in a delta-front area. The  
313 parallel orientation of the inclined beds and the cross-bedding indicates forward accretion.  
314 The alternating finer and coarser beds are interpreted to reflect fluctuations in river discharge  
315 that, together with the unidirectional, seaward-oriented palaeocurrents, indicate river  
316 dominance, although heterolithic deposits with rhythmically-distributed mudstone drapes and  
317 bidirectional ripples suggest subordinate tidal influence. FA 6 differs from FA 4 in size and in  
318 grain sorting. The mouth-bar deposits of FA 6 are interpreted to be distal features of major  
319 distributary channels (FA 1), and therefore had more time for sediment to move downstream  
320 to become overall finer. In contrast, the crevasse delta mouth bars have a coarser grain size  
321 that reflects their more proximal position in the system. The higher mud content in FA 4  
322 reflects the overall lower-energy setting and higher turbidity present in interdistributary bays  
323 relative to mouth bars in an exposed frontal location (Gugliotta et al. 2015).

324

325 *FA 7: Interdistributary-bay and prodelta mudstones*

326 Description: FA 7 consists of blue to grey mudstones lacking any internal structures, with  
327 sandstone and coarse siltstone layers from a few millimetres to 0.1 m thick. Units are tabular,  
328 up to several tens of m thick and extend up to several kilometres laterally. FA 7 is  
329 gradationally overlain by FA 4 or FA 6 and is associated with FA 8. Trace-fossil abundance  
330 is generally high (BI 5-6).

331

332 Interpretation: FA 7 is interpreted as interdistributary-bay and prodelta deposits rather than  
333 open-shelf offshore mudstones because of the lateral association with FA 4 and FA 6, and the

334 lack of open-marine indicators such as a pelagic fauna (e.g. ammonites, belemnites) or  
335 carbonates. FA 7 formed mainly from suspension fallout away from the main distributary  
336 channels and in the distal part of the delta system. Thin sandstone and coarse siltstone beds  
337 are interpreted as episodic depositional events marking large river floods. The lack of  
338 lamination is probably due to complete or almost complete bioturbation (BI 5-6), which  
339 suggests the presence of relatively more persistent brackish-water to fully marine conditions,  
340 with long periods of slow to negligible deposition.

341

342 *FA 8: Transgressive and abandonment deposits*

343 Description: FA 8 consists of a variety of siliciclastic and carbonate deposits that usually cap  
344 coarsening-upward units of FA 6, but can also overlie all of the other facies associations.  
345 These units are commonly laterally extensive, being traceable for distances of up to several  
346 kilometres, although they can also extend for only a few tens of metres in other cases.  
347 Siliciclastic deposits consist of sandstone beds up to 0.4 m thick that contain hummocky  
348 cross-stratification or dune-scale bedforms up to 1.5 m high. Carbonate deposits consist of  
349 shell-beds containing corals, oysters, echinoderms, *Trigonia*, brachiopods and other  
350 undifferentiated shells. Shells are usually well preserved and consist of articulated and  
351 disarticulated valves. Beds composed of broken shells are rare. Shell beds overlying delta  
352 plain deposits (FA 2, FA 3, FA 4 and FA 7) are commonly composed exclusively of oysters  
353 whereas those overlying delta front deposits (FA 5, FA 6, FA 7) contain a more diverse  
354 range of shells.

355

356 Interpretation: Both carbonate and siliciclastic deposits in FA 8 are interpreted as brackish to  
357 fully marine facies that sharply overlie, and are in turn overlain by, shallower-water deposits  
358 (such as interdistributary bay, mouth bar or prodelta facies). Shells can be preserved *in situ*

359 (articulated) or have been subjected to minor transport and reworking (disarticulated valves).  
360 The carbonate shell beds are interpreted as lags accumulated during times of low siliciclastic  
361 input that allowed a benthic invertebrate fauna to thrive (Fuersich and Oschmann 1993).  
362 Shell-beds composed of broken shells are interpreted as storm deposits. The dunes composed  
363 of reworked sand, are known to be common on transgressive surfaces (Correggiari et al.  
364 1996), whereas hummocky cross-stratification implies a general deepening of water and an  
365 increase in wave fetch. FA 8 is interpreted as marine sediments associated with regional  
366 flooding surfaces or local abandonment of the deltaic lobes.

367

### 368 **Fluctuation of fluvial discharge and tidal signals**

#### 369 *Interbedding: description*

370 The coarser-grained beds described in FA 1, FA 3, FA 4 and FA 6 show a high degree of  
371 variability in their detailed characteristics, but also share many affinities (Fig. 8). Typically,  
372 the coarser-grained beds have erosional bases, can contain mudstone clasts and are  
373 structureless or show seaward-directed, unidirectional trough or planar-tabular dune-scale  
374 cross-stratification and current-ripple cross-lamination. Locally, these beds contain cyclical  
375 carbonaceous drapes on dune foresets, but these are not common. The trace-fossil content is  
376 absent or extremely low (BI 0-1) and generally of low diversity. Contacts are gradational  
377 with the overlying finer-grained sandstones and siltstones that may contain mudstone or  
378 carbonaceous and/or mica drapes, forming mm-scale cyclical rhythmites. These rhythmites  
379 rarely show cyclical patterns and can be associated with bidirectional ripples. A more  
380 abundant and diverse suite of trace fossils (e.g. *Palaeophycus*, *Ophiomorpha*, *Dactyloidites*,  
381 *Thalassinoides*, *Planolites*) is present compared to coarser-grained beds and is associated  
382 with an increase in the size of burrows. The intensity of bioturbation can be either low (BI 2-  
383 3) or can obliterate all sedimentary structures (BI 5-6; Fig. 7D, E). Some examples show the

384 trace fossils extending downwards into the underlying coarser beds. Alternatively, the finer-  
385 grained intervening bed may show high concentrations of carbonaceous matter (Fig. 4B).

386

387 *Interbedding: interpretation*

388 The sandstone beds with erosional bases and unidirectional, offshore-directed palaeocurrents  
389 are interpreted as the deposits of river floods, which formed under strongly or entirely fluvial  
390 conditions. The rare rhythmic carbonaceous drapes may be the result of a tidal modulation of  
391 the river flow (Martinius and Gowland 2011), which would nevertheless imply a dominance  
392 of river currents as such tidal modulation of unidirectional river flow is inferred to occur in  
393 the inner part of the fluvial to marine transition zone (Dalrymple and Choi 2007; Dashtgard et  
394 al. 2012). The intervening, finer-grained beds with bidirectional ripples, cyclical rhythmites,  
395 and increased bioturbation levels are interpreted as interflood deposits formed during low  
396 river stage and under short-term dominance of tidal processes and brackish to fully marine  
397 conditions. Cyclical patterns are similar to those described in tidal deposits (De Boer et al.  
398 1989). Rare top-down burrows in the coarser beds originated from the interflood beds,  
399 suggesting a stronger marine influence during low river stage. The abundance of  
400 carbonaceous material in the interflood deposits is interpreted as a sign of low river energy,  
401 because of the hydraulically light nature of the fine-grained “tea leaves” that comprise the  
402 organic detritus.

403

404 *Additional indicators of river discharge fluctuations*

405 The sedimentary facies described above provide process-based indications that significant  
406 variations in river discharge are recorded in the deposits. Other features can be used to  
407 support this interpretation although these features alone are insufficient to prove the impact  
408 that river discharge fluctuations had on sedimentation. In general, the trace fossils in the

409 Lajas Fm. show low numbers of infaunal populations, which suggest a stressed environment  
410 (MacEachern et al. 2010). This is possibly the result of low and variable salinity and  
411 inconstant discharge, although it has been previously associated with temperature stress  
412 (McIlroy et al. 2005). Also, the ichnotaxa *Dactyloidites* is common in many of these deposits,  
413 typically as a monospecific assemblage. This is the trace of an opportunistic colonizer,  
414 mainly found in river-dominated deltas. It is commonly associated with rapid, episodic  
415 sedimentation, the presence of organic matter and high turbidity in the water column  
416 (Agirrezabala and de Gibert 2004). These conditions are fully consistent with the  
417 interpretation of variable river discharge. Synaeresis cracks are also present in the Lajas Fm.  
418 (Fig. 4E). They form because high discharge events during river floods may lead to the  
419 temporary introduction of reduced-salinity waters immediately above the sediment–water  
420 interface (MacEachern et al. 2010).

421

## 422 **Discussion**

### 423 *Seasonal discharge variations in the Lajas Fm.*

424 The studied portions of the Lajas Fm. show decimetre-scale interbedded coarser-grained beds  
425 (river flood deposits) and finer-grained beds with tidal affinity (interflood deposits). The  
426 alternations of these two types of bed create non-cyclic rhythmites that are interpreted to be  
427 the result of variations in river discharge. This is because the magnitude of river floods varies  
428 stochastically, rather than cyclically and predictably like tides. This interpreted fluvial  
429 signature is present in a variety of deposits ranging from distal (mouth bar deposits, FA 6) to  
430 more proximal facies such as the point bars of fluvial and distributary channels (FA 1). The  
431 presence of preserved bar deposits suggests seasonal rather than ephemeral rivers because  
432 barforms are commonly reworked and cannibalised in ephemeral systems (Fielding et al.  
433 2009; Fielding et al. 2011; Wilson et al. 2014). Key characteristics of channels with flashy

434 discharge, such as abundant, pedogenically modified mud partings, abundance of upper-flow-  
435 regime sedimentary structures and *in situ* trees (Fielding 2006; Fielding et al. 2009; Fielding  
436 et al. 2011; Gulliford et al. 2014; Wilson et al. 2014) are missing from the Lajas Formation.  
437 The high levels of bioturbation (commonly BI 4-6) and the increased size of burrows in the  
438 interflood beds suggests that it would take burrowers at least several months to re-establish  
439 the degree of bioturbation to such a high level after a flooding event, if they were emplaced  
440 by larvae (Gingras et al. 2002; Gingras and MacEachern 2012). This pattern of bioturbation  
441 intensity supports the interpretation of a seasonal origin for the beds. Furthermore, because of  
442 the relatively large size of the river channels (sand bodies up to 12 m thick) and the location  
443 of the source area, the Sierra Pintada belt and the Patagonian Massif (Fig. 2), both of which  
444 are located at least 100 km away (Uliana and Legarreta 1993), the Lajas Fm. rivers likely  
445 drained large catchments that were able to absorb local precipitation and therefore primarily  
446 record seasonal discharge fluctuations.

447

448 *Fluvial versus tidal control on the bedding of the Lajas Fm.*

449 As highlighted in the introduction, heterolithic deposits are often considered tidal in origin.  
450 Semidiurnal or diurnal cycles are required to account for mm-scale interlamination that is  
451 visible in the fine-grained, interflood beds. A tidal origin for the decimetre-scale interbedding  
452 of coarser- and finer-grained deposits would require the operation of a longer duration tidal  
453 periodicity, such as neap-spring cycles. However, this assertion does not fit with the almost  
454 total absence of a clear tidal signal within the coarser-grained beds (Fig. 8). If these beds  
455 were deposited during spring tides, it might be expected that the tidal signal would be more  
456 strongly developed in them rather than in the intervening, fine-grained neap-tide deposit. This  
457 is because spring tides are stronger and able to entrain more mud into suspension than neap  
458 tides, which could result in more pronounced cyclical rhythmities and therefore a clearer tidal

459 signal in the spring-tide deposits (Nio and Yang 1991). By the same principles, if formed  
460 under spring-tidal periods, landward-oriented and bidirectional cross-stratification and cross-  
461 lamination would be more common in the sandstone beds than in the intervening deposits, in  
462 contrast with our observations that the tidal signal is most pronounced in the fine-grained  
463 beds. Alternatively, a single coarser-grained bed could theoretically be considered as the  
464 result of a single tidal phase (flood or ebb); however, because of the short duration of a single  
465 phase of the tide, the thickness of a sand layer that can be deposited by a single tide is  
466 limited. Published results from modern and ancient tidal rhythmites (De Boer et al. 1989;  
467 Dalrymple et al. 1991; Archer 1995; Kvale et al. 1995; Archer 1996; Mazumder and Arima  
468 2005; Choi 2011; Dalrymple et al. 2012; Kvale 2012; Longhitano et al. 2012; Johnson and  
469 Dashtgard 2014) suggest that the deposit of a single tidal phase is commonly less than 2-3 cm  
470 in thickness (and rarely above 5 cm), and thus thinner than most of the sand beds described  
471 herein.

472 In our interpretation, evidence for river discharge variations and tidal processes are both  
473 present in the Lajas Fm. deposits, but they can be decoupled. The seasonal fluctuations of the  
474 river discharge are interpreted to be the controlling influence on sedimentation. They produce  
475 a change in strength and regime of the fluvial current, which is reflected in the distinct  
476 alternation of coarser- and finer-grained beds. This interpretation is supported by the absence  
477 of a cyclical pattern in the coarser-grained beds (river floods) and the seaward orientation of  
478 cross-stratification. Furthermore, the regular alternation of burrowed and unburrowed layers  
479 in marginal-marine deposits have also been associated with seasonal variations in  
480 sedimentary conditions (Gingras and MacEachern 2012).

481 The waxing phase of the river flood period is responsible for the development of the basal  
482 erosion surface of each coarse-grained bed (Fig. 9A). Deposition starts during the waning  
483 stage of the river flood (Bridge 2003) when the coarser-grained bed is formed under fluvial-

484 dominated conditions (Fig. 9B). Waning river energy during the late stage of the river flood  
485 results in deposition of finer grain sizes and subordinate modification by tidal currents (Fig.  
486 9C). Finally, during the interflood period at low river stage, sediment is reworked by tidal  
487 processes (Fig. 9D).

488

489 *Distribution and trends of seasonal and tidal deposits: facies control on preservation*

490 Seasonal bedding is interpreted to be present in the Lajas Fm. in mouth-bar deposits (FA 6),  
491 crevasse-mouth-bar deposits (FA 4) and both point bars and side-attached bars within major  
492 and minor channel deposits (FA 1 and 3; Fig. 10). In the upper (proximal) part of crevasse-  
493 mouth-bar units, river flood beds are thicker and more amalgamated than in the lower section  
494 of the body. This is interpreted as due to erosion of interflood beds by strong river currents at  
495 high river stage. River flood-interflood couplets are well-developed in the medial part of  
496 mouth bars because river flood erosion is less significant, but they become less well-  
497 developed in the distal part of the crevasse mouth bar because of tidal and biological  
498 reworking during interflood periods (Gugliotta et al., 2015). A similar pattern is visible also  
499 in main mouth-bar deposits (FA 6), which show a similar upward trend of decreasing  
500 preservation of interbedding and lack of interflood beds in the top part, where river flood  
501 beds are thicker and more amalgamated (Fig. 10).

502 In the channel deposits, seasonal bedding is poorly-developed in the channel thalweg because  
503 of the high energy erosion during river floods but is well developed in side-bar and point-bar  
504 deposits of FA 1 and FA 3 (i.e. in areas that are more strongly depositional; Fig. 10).  
505 Terminal distributary channels (FA 5) do not show clear seasonal bedding also because of the  
506 strongly erosive conditions therein. Channel thalweg deposits are dominated by the presence  
507 of dunes and some of them show evidence for a tidal signature (i.e. rhythmically distributed  
508 carbonaceous drapes; Fig. 5), but they do not show a clear sign of seasonality. Although the

509 life-span of dunes is poorly constrained, it is considered unlikely that a single cross-bed  
510 would record one complete year of deposition or let alone several years, because of the  
511 erosion of the stoss side as the dune migrates. In the case that deposition occurs continuously,  
512 modern fluvial and tidal dunes have migration rates on the order of tens of centimetres to tens  
513 of metres per day (Visser 1980; Van Den Berg 1987; Dalrymple and Rhodes 1995; Harbor  
514 1998; Villard and Church 2003; Martinius and Gowland 2011). Assuming that the seasonal  
515 control will be due to annual changes in river discharge and that at least a few cycles are  
516 required to permit recognition, a single cross bed would have to be exposed continuously  
517 over a distance of hundreds to thousands of metres, something that is highly unlikely to exist.  
518 A tidal modulation cycle, that is needed to produce cyclically-distributed carbonaceous  
519 drapes, lasts only 6 or 12 hours, depending on whether the system is semi-diurnal or diurnal,  
520 and could be recorded in a few metres of continuous sedimentation. This implies that some  
521 facies will tend to record preferentially one process rather than another (in this case tides  
522 rather than seasonality). However, this does not mean that the tidal signal is the main control  
523 on deposition in the entire environment. To avoid misinterpretation we need to base our  
524 evaluation on examination of the whole system rather than on a single facies.

525 Other deposits described in this paper show little or no evidence of seasonal bedding; these  
526 include all of the mud-rich deltaic deposits, such as floodplain (FA 2) and interdistributary  
527 bay-mud and prodelta deposits (FA 7). The reason why seasonal bedding is not present in  
528 these facies associations is ascribed to the lack or sporadic nature of sand input in these distal,  
529 low-energy areas and/or obliteration of all bedding by bioturbation. In transgressive deposits  
530 (FA 8) seasonal bedding is not developed because these deposits form in distal settings, far  
531 removed from the influence of the river.

532 The preservation of seasonal bedding in the Lajas Fm. is strongly facies controlled. Seasonal  
533 deposits are present only in facies that form under steady rates of sedimentation over several

534 seasons with little erosion. These conditions are usually met in bars that form both within  
535 (side bars and point bars) and at the mouth (crevasse mouth bars and mouth bars) of channels.  
536 Thus, the basic conditions needed to preserve seasonal bedding are: 1) presence of seasonal  
537 discharge in the river (which is the norm in modern rivers); 2) relatively continuous local  
538 sedimentation and little erosion during river flood periods (such conditions occur commonly  
539 on bars); and 3) relatively little reworking by tidal, wave and biological processes.

540

#### 541 **Conclusions**

542 The studied deposits of the Lajas Formation comprise delta mouth bar, distributary channel  
543 and a range of delta plain deposits. Major and minor channel and mouth bar deposits show a  
544 ubiquitous decimetre-scale interbedding of coarser-grained beds (river flood) and finer-  
545 grained beds (interflood) that form non-cyclic rhythmites. River flood beds have  
546 unidirectional seaward-directed palaeocurrents and little evidence of tidal processes and  
547 brackish water conditions. Interflood beds show evidence of tidal process (tidal rhythmites,  
548 bidirectional palaeocurrents) and of brackish water conditions (trace fossils). The  
549 interpretation of the rhythmites is that they record variations in river discharge rather than  
550 tides because the magnitude of river floods is stochastic and does not vary regularly, whereas  
551 tides are cyclical and predictable. The deposit of a single tidal phase would be thinner than  
552 most of the river-flood deposits described herein and the almost total absence of a clear tidal  
553 signal in the coarser-grained beds would exclude their origin from a longer duration tidal  
554 cyclicity. Moreover, regular alternation of burrowed and unburrowed layers, like those  
555 described herein, has commonly been associated with seasonal variations in sedimentary  
556 conditions.

557 The characteristics and distribution of the bedding suggest a seasonal pattern rather than the  
558 shorter-term and more drastic fluctuations associated with flashy river discharge. Seasonal

559 patterns of deposition from perennial rivers should represent the norm and not the exception  
560 in coast-zone rivers, because seasonal discharge fluctuations are a fundamental process in  
561 present day river systems worldwide and are expected to be preserved in the large part of  
562 ancient fluvial and deltaic deposits (Fig. 1).

563 The occurrence of seasonal deposits in the Lajas Fm. is facies controlled, and preferentially  
564 preserved in areas with relatively continuous sedimentation and limited erosion, such as on  
565 bars that form within or at the mouth of major and minor channels. The seasonal signal is not  
566 preserved where river flood processes are too powerful and remove the interflood deposits,  
567 such as in channel thalwegs and terminal distributary channels, or where the river input is  
568 weak and sporadic, such as in floodplain, muddy interdistributary bay, prodelta and  
569 transgressive marine deposits. Some facies, such as dunes, can record tidal modulation rather  
570 than seasonality; this must be taken into account in the evaluation of the main control on  
571 deposition. Consequently, to avoid misinterpretations, the evaluation of the dominant process  
572 in similar types of ancient deposits should be based on the whole system rather than on a  
573 single facies or facies association.

574

#### 575 **Acknowledgments**

576 This work is part of the LAJAS Project, a joint study by the Universities of Manchester (UK),  
577 Leeds (UK), La Plata (Argentina), University of Texas at Austin (USA) and Queen's  
578 University, Ontario (Canada). The project is sponsored by BHPBilliton, Statoil, VNG Norge  
579 and Woodside, who are acknowledged for financial support. Allard Martinius and an  
580 anonymous reviewer are acknowledged for their comments, which have helped to improve  
581 the manuscript. The authors would like to thank Luciano Zapata, Rachel Harding, Brian  
582 Burnham, Geoff Reith and Thomas Maguire for assistance in the field, Gonzalo Veiga for

583 insights into the Neuquén Basin and the farmers of Los Molles area for kindly allowing  
584 access onto their lands.

585

586 **References**

587 Agirrezabala, L.M. & de Gibert, J.M. 2004. Paleodepth and paleoenvironment of *Dactyloidites ottoi*  
588 (Geinitz, 1849) from Lower Cretaceous deltaic deposits (Basque-Cantabrian Basin, west Pyrenees).

589 *Palaios*, **19**, 276-291.

590 Allen, G.P. & Chambers, J.L. 1998. Sedimentation in the modern and Miocene Mahakam Delta.

591 Indonesian Petroleum Association, 236.

592 Allen, G.P., Salomon, J.C., Bassoullet, J.P., Du Penhoat, Y. & De Grandpre, C. 1980. Effects of tides on  
593 mixing and suspended sediment transport in macrotidal estuaries. *Sedimentary Geology*, **26**, 69-90.

594 Allen, J.R.L. 1981. Lower Cretaceous tides revealed by cross-bedding with mud drapes. *Nature*  
595 (*London*), **289**, 579-581.

596 Archer, A.W. 1995. Modeling of cyclic tidal rhythmites based on a range of diurnal to semidiurnal  
597 tidal-station data. *Marine Geology*, **123**, 1-10.

598 Archer, A.W. 1996. Reliability of lunar orbital periods extracted from ancient cyclic tidal rhythmites.

599 *Earth and Planetary Science Letters*, **141**, 1-10, doi: 10.1016/0012-821x(96)00063-5.

600 Brandsaeter, I., McIlroy, D., Lia, O., Ringrose, P.S. & Naess, A. 2005. Reservoir modelling and  
601 simulation of Lajas Formation outcrops (Argentina) to constrain tidal reservoirs of the Halten Terrace

602 (Norway). *Petroleum Geoscience*, **11**, 37-46, doi: 10.1144/1354-079303-611.

603 Bridge, J.S. 2003. Rivers and floodplains; forms, processes, and sedimentary record. Blackwell  
604 Publishing, Oxford, United Kingdom, 504.

605 Choi, K. 2010. Rhythmic climbing-ripple cross-lamination in inclined heterolithic stratification (IHS) of  
606 a macrotidal estuarine channel, Gomso Bay, west coast of Korea. *Journal of Sedimentary Research*,

607 **80**, 550-561, doi: 10.2110/jsr.2010.054.

608 Choi, K. 2011. External controls on the architecture of inclined heterolithic stratification (IHS) of  
609 macrotidal Sukmo Channel; wave versus rainfall. *Marine Geology*, **285**, 17-28, doi:  
610 10.1016/j.margeo.2011.05.002.

611 Correggiari, A., Field, M.E. & Trincardi, F. 1996. Late Quaternary transgressive large dunes on the  
612 sediment-starved Adriatic Shelf. *Geological Society Special Publications*, **117**, 155-169.

613 Dalrymple, R.W. 2010. Tidal depositional systems. In: James, N.P. & Dalrymple, R.W. (eds.) *Facies*  
614 *Models 4*. Geological Association of Canada, 201-231.

615 Dalrymple, R.W. & Choi, K. 2007. Morphologic and facies trends through the fluvial-marine transition  
616 in tide-dominated depositional systems; a schematic framework for environmental and sequence  
617 stratigraphic interpretation. *Earth-Science Reviews*, **81**, 135-174, doi:  
618 10.1016/j.earscirev.2006.10.002.

619 Dalrymple, R.W., Mackay, D.A., Ichaso, A.A. & Choi, K.S. 2012. Processes, morphodynamics, and  
620 facies of tide-dominated estuaries. In: Davis, R.A.J. & Dalrymple, R.W. (eds.) *Principles of Tidal*  
621 *Sedimentology*. Springer Berlin, 79-107.

622 Dalrymple, R.W., Makino, Y. & Zaitlin, B.A. 1991. Temporal and spatial patterns of rhythmite  
623 deposition on mud flats in the macrotidal Cobequid Bay-Salmon River estuary, Bay of Fundy, Canada.

624 Dalrymple, R.W. & Rhodes, R.N. 1995. Estuarine dunes and bars. *Amsterdam, Elsevier, Developments*  
625 *in sedimentology*, **53**, 359-422.

626 Dalrymple, R.W., Zaitlin, B.A. & Boyd, R. 1992. Estuarine facies models: conceptual basis and  
627 stratigraphic implications. *Journal of Sedimentary Petrology*, **62**, 1130-1146.

628 Dark, P. & Allen, J.R.L. 2005. Seasonal deposition of Holocene banded sediments in the Severn  
629 Estuary Levels (southwest Britain): palynological and sedimentological evidence. *Quaternary Science*  
630 *Reviews*, **24**, 11-33, doi: 10.1016/j.quascirev.2004.08.001.

631 Dashtgard, S.E., Venditti, J.G., Hill, P.R., Sisulak, C.F., Johnson, S.M. & La Croix, A.D. 2012.  
632 Sedimentation across the tidal-fluvial transition in the Lower Fraser River, Canada. *SEPM, The*  
633 *Sedimentary Record*, **10**, 4-9.

634 Davis, R., Jr. 2012. Tidal Signatures and Their Preservation Potential in Stratigraphic Sequences. *In:*  
635 Davis Jr, R.A. & Dalrymple, R.W. (eds.) *Principles of Tidal Sedimentology*. Springer Berlin, 35-55.

636 De Boer, P.L., Oost, A.P. & Visser, M.J. 1989. The diurnal inequality of the tide as a parameter for  
637 recognizing tidal influences. *Journal of Sedimentary Petrology*, **59**, 912-921, doi: 10.1306/212f90b1-  
638 2b24-11d7-8648000102c1865d.

639 Fielding, C.R. 2006. Upper flow regime sheets, lenses and scour fills; extending the range of  
640 architectural elements for fluvial sediment bodies. *Sedimentary Geology*, **190**, 227-240, doi:  
641 10.1016/j.sedgeo.2006.05.009.

642 Fielding, C.R. & Alexander, J. 1996. Sedimentology of the Upper Burdekin River of North Queensland,  
643 Australia—an example of a tropical, variable discharge river. *Terra Nova*, **8**, 447-457, doi:  
644 10.1111/j.1365-3121.1996.tb00770.x.

645 Fielding, C.R., Allen, J.P., Alexander, J. & Gibling, M.R. 2009. Facies model for fluvial systems in the  
646 seasonal tropics and subtropics. *Geology (Boulder)*, **37**, 623-626, doi: 10.1130/g25727a.1.

647 Fielding, C.R., Allen, J.P., Alexander, J., Gibling, M.R., Rygel, M.C. & Calder, J.H. 2011. Fluvial systems  
648 and their deposits in hot, seasonal semi-arid and sub-humid settings; modern and ancient examples.  
649 *Special Publication - Society for Sedimentary Geology*, **97**, 89-111.

650 Fuersich, F.T. & Oschmann, W. 1993. Shell beds as tools in basin analysis; the Jurassic of Kachchh,  
651 western India. *Journal of the Geological Society of London*, **150**, 169-186.

652 Garcia, V.M., Quattrocchio, M.E., Zavala, C.A. & Martinez, M.A. 2006. Palinofacies, paleoambientes y  
653 paleoclima del Grupo Cuyo (Jurásico Medio) en la Sierra de Chacaico, Cuenca Neuquina, Argentina.  
654 *Revista Espanola de Micropaleontologia*, **38**, 269-288.

655 Geel, C.R. & Donselaar, M.E. 2007. Reservoir modelling of heterolithic tidal deposits; sensitivity  
656 analysis of an object-based stochastic model. *Geologie en Mijnbouw. Netherlands Journal of*  
657 *Geosciences*, **86**, 403-411.

658 Gingras, M.K. & MacEachern, J.A. 2012. Tidal ichnology of shallow-water clastic settings. *In:* Davis Jr,  
659 R.A. & Dalrymple, R.W. (eds.) *Principles of Tidal Sedimentology*. Springer, Berlin, 57-77.

660 Gingras, M.K., Rasanen, M. & Ranzi, A. 2002. The significance of bioturbated inclined heterolithic  
661 stratification in the southern part of the Miocene Solimoes Formation, Rio Acre, Amazonia Brazil.  
662 *Palaios*, **17**, 591-601.

663 Gonzalez-Hidalgo, J.C., Batalla, R.J. & Cerda, A. 2013. Catchment size and contribution of the largest  
664 daily events to suspended sediment load on a continental scale. *Catena (Giessen)*, **102**, 40-45, doi:  
665 10.1016/j.catena.2010.10.011.

666 Gonzalez-Hidalgo, J.C., Batalla, R.J., Cerda, A. & de Luis, M. 2010. Contribution of the largest events  
667 to suspended sediment transport across the USA. *Land Degradation and Development*, **21**, 83-91,  
668 doi: 10.1002/ldr.897.

669 Gugliotta, M., Flint, S.S., Hodgson, D.M. & Veiga, G.D. 2015. Stratigraphic Record of River-Dominated  
670 Crevasse Subdeltas With Tidal Influence (Lajas Formation, Argentina). *Journal of Sedimentary*  
671 *Research*, **85**, 265-284, doi: 10.2110/jsr.2015.19.

672 Gulliford, A.R., Flint, S.S. & Hodgson, D.M. 2014. Testing applicability of models of distributive fluvial  
673 systems or trunk rivers in ephemeral systems; reconstructing 3-D fluvial architecture in the Beaufort  
674 Group, South Africa. *Journal of Sedimentary Research*, **84**, 1147-1169, doi: 10.2110/jsr.2014.88.

675 Harbor, D.J. 1998. Dynamics of bedforms in the lower Mississippi River. *Journal of Sedimentary*  
676 *Research*, **68**, 750-762, doi: 10.2110/jsr.68.750.

677 Howell, J.A., Schwarz, E., Spalletti, L.A. & Veiga, G.D. 2005. The Neuquen Basin: an overview. In:  
678 Veiga, G.D., Spalletti, L.A., Howell, J.A. & Schwartz, E. (eds.) *The Neuquén Basin, Argentina: A Case*  
679 *Study in Sequence Stratigraphy and Basin Dynamics*. Geological Society of London, London, United  
680 Kingdom, Geological Society of London, Special Publication, 1-14.

681 Ichaso, A.A. & Dalrymple, R.W. 2009. Tide- and wave-generated fluid mud deposits in the Tilje  
682 Formation (Jurassic), offshore Norway. *Geology (Boulder)*, **37**, 539-542, doi: 10.1130/g25481a.1.

683 Iglesia Llanos, M.P. 2012. Palaeomagnetic study of the Jurassic from Argentina: magnetostratigraphy  
684 and palaeogeography of South America. *Revue de Paleobiologie*, 151-168.

685 Iglesia Llanos, M.P., Riccardi, A.C. & Singer, S.E. 2006. Palaeomagnetic study of Lower Jurassic marine  
686 strata from the Neuquen Basin, Argentina: a new Jurassic apparent polar wander path for South  
687 America. *Earth and Planetary Science Letters*, **252**, 379-397, doi: 10.1016/j.epsl.2006.10.006.

688 Johnson, S.M. & Dashtgard, S.E. 2014. Inclined heterolithic stratification in a mixed tidal–fluvial  
689 channel: Differentiating tidal versus fluvial controls on sedimentation. *Sedimentary Geology*, **301**, 41-  
690 53, doi: <http://dx.doi.org/10.1016/j.sedgeo.2013.12.004>.

691 Kravtsova, V.I., Mikhailov, V.N. & Kidyayeva, V.M. 2009. Hydrological regime, morphological features  
692 and natural territorial complexes of the Irrawaddy River Delta (Myanmar). *Water Resources*, **36**, 243-  
693 260, doi: 10.1134/s0097807809030014.

694 Kurcinka, C.E. 2014. *Sedimentology and facies architecture of the tide-influenced, river-dominated*  
695 *delta-mouth bars in the lower Lajas Fm (Jurassic), Argentina*. unpublished MSc thesis, Queen’s  
696 University, 157.

697 Kvale, E. 2012. Tidal Constituents of Modern and Ancient Tidal Rhythmites: Criteria for Recognition  
698 and Analyses. In: Davis Jr, R.A. & Dalrymple, R.W. (eds.) *Principles of Tidal Sedimentology*. Springer,  
699 Berlin, 1-17.

700 Kvale, E.P., Cutright, J., Blodeau, D., Archer, A., Johnson, H.R. & Pickett, B. 1995. Analysis of modern  
701 tides and implications for ancient tidalites. *Continental Shelf Research*, **15**, 1921-1943.

702 La Croix, A.D. & Dashtgard, S.E. 2014. Of sand and mud: Sedimentological criteria for identifying the  
703 turbidity maximum zone in a tidally influenced river. *Sedimentology*, **61**, 1961-1981, doi:  
704 10.1111/sed.12126.

705 Legler, B., Johnson, H.D., Hampson, G.J., Massart, B.Y.G., Jackson, C.A.L., Jackson, M.D., El-Barkooky,  
706 A. & Ravnas, R. 2013. Facies model of a fine-grained, tide-dominated delta: Lower Dir Abu Lifa  
707 Member (Eocene), Western Desert, Egypt. *Sedimentology*, 1313–1356, doi: 10.1111/sed.12037.

708 Longhitano, S.G., Mellere, D., Steel, R.J. & Ainsworth, R.B. 2012. Tidal depositional systems in the  
709 rock record: a review and new insights. *Sedimentary Geology*, **279**, 2-22, doi:  
710 10.1016/j.sedgeo.2012.03.024.

711 MacEachern, J.A., Pemberton, S.G., Gingras, M.K. & Bann, K.L. 2010. Ichnology and facies models. *In:*  
712 James, N.P. & Dalrymple, R.W. (eds.) *Facies Models 4*. Geological Association of Canada, 19-58.

713 MacKay, D.A. & Dalrymple, R.W. 2011. Dynamic mud deposition in a tidal environment; the record of  
714 fluid-mud deposition in the Cretaceous Bluesky Formation, Alberta, Canada. *Journal of Sedimentary*  
715 *Research*, **81**, 901-920, doi: 10.2110/jsr.2011.74.

716 Martinez, M.A., Quattrocchio, M.E. & Zavala, C.A. 2002. Análisis palinofacial de la Formación Lajas  
717 (Jurásico Medio), Cuenca Neuquina, Argentina: significado paleoambiental y paleoclimático. *Revista*  
718 *Espanola de Micropaleontologia*, **34**, 81-104.

719 Martinius, A.W. & Gowland, S. 2011. Tide-influenced fluvial bedforms and tidal bore deposits (Late  
720 Jurassic Lourinha Formation, Lusitanian Basin, western Portugal). *Sedimentology*, **58**, 285-324, doi:  
721 10.1111/j.1365-3091.2010.01185.x.

722 Martinius, A.W., Ringrose, P.S., Brostrom, C., Elfenbein, C., Naess, A. & Ringas, J.E. 2005. Reservoir  
723 challenges of heterolithic tidal sandstone reservoirs in the Halten Terrace, mid-Norway. *Petroleum*  
724 *Geoscience*, **11**, 3-16, doi: 10.1144/1354-079304-629.

725 Martinius, A.W. & Van den Berg, J.H. 2011. Atlas of sedimentary structures in estuarine and tidally-  
726 influenced river deposits of the Rhine-Meuse-Scheldt system: Their application to the interpretation  
727 of analogous outcrop and subsurface depositional systems. EAGE Publications, Houten, 298

728 Mazumder, R. & Arima, M. 2005. Tidal rhythmites and their implications. *Earth-Science Reviews*, **69**,  
729 79-95.

730 McIlroy, D., Flint, S. & Howell, J.A. 1999. Sequence stratigraphy and facies architecture of tidal  
731 succession, in an extensional basin; Neuquén Basin, Argentina. *American Association of Petroleum*  
732 *Geologists, Annual Meeting Expanded Abstracts*, **1999**, A91-A92.

733 McIlroy, D., Flint, S., Howell, J.A. & Timms, N. 2005. Sedimentology of the tide-dominated Jurassic  
734 Lajas Formation, Neuquén Basin, Argentina. *In:* Veiga, G.D., Spalletti, L.A., Howell, J.A. & Schwartz, E.  
735 (eds.) *The Neuquén Basin, Argentina: A Case Study in Sequence Stratigraphy and Basin Dynamics*.  
736 Geological Society of London, Special Publications, 83-107.

737 Mikhailov, V.N. & Mikhailova, M.V. 2010. Delta formation processes at the Mississippi River mouth.  
738 *Water Resources*, **37**, 595-610, doi: 10.1134/s0097807810050015.

739 Milliman, J.D. & Farnsworth, K.L. 2011. River discharge to the coastal ocean: a global synthesis,  
740 Cambridge University Press, 392.

741 Morgans-Bell, H.S. & McIlroy, D. 2005. Palaeoclimatic implications of Middle Jurassic (Bajocian)  
742 coniferous wood from the Neuquen Basin, west-central Argentina. *In*: Veiga, G.D., Spalletti, L.A.,  
743 Howell, J.A. & Schwartz, E. (eds.) *The Neuquén Basin, Argentina: A Case Study in Sequence*  
744 *Stratigraphy and Basin Dynamics*. Geological Society of London, Special Publication, 267-278.

745 Nio, S.-D. & Yang, C. 1991. Diagnostic attributes of clastic tidal deposits; a review. *Memoir - Canadian*  
746 *Society of Petroleum Geologists*, **16**, 3-27.

747 Nordahl, K., Martinius, A.W. & Kritski, A. 2006. Time-series analysis of a heterolithic, ripple-  
748 laminated deposit (Early Jurassic, Tilje Formation) and implications for reservoir modelling. *Marine*  
749 *Geology*, **235**, 255-271, doi: 10.1016/j.margeo.2006.10.019.

750 Olariu, C. & Bhattacharya, J.P. 2006. Terminal distributary channels and delta front architecture of  
751 river-dominated delta systems. *Journal of Sedimentary Research*, **76**, 212-233, doi:  
752 10.2110/jsr.2006.026.

753 Plink-Björklund, P. 2012. Effects of tides on deltaic deposition: Causes and responses. *Sedimentary*  
754 *Geology*, **279**, 107-133.

755 Purnachandra Rao, V., Shynu, R., Kessarkar, P.M., Sundar, D., Michael, G.S., Narvekar, T., Blossom, V.  
756 & Mehra, P. 2011. Suspended sediment dynamics on a seasonal scale in the Mandovi and Zuari  
757 Estuaries, central west coast of India. *Estuarine, Coastal and Shelf Science*, **91**, 78-86, doi:  
758 10.1016/j.ecss.2010.10.007.

759 Quattrocchio, M., Garcia, V., Martinez, M. & Zavala, C. 2001. A hypothetic scenario for the Middle  
760 Jurassic in the southern part of the Neuquén Basin, Argentina. *Asociación Paleontológica Argentina*,  
761 *Publicacion Especial*, **7**, 163-166.

762 Rebata, H., Luisa A., Gingras, M.K., Rasanen, M.E. & Barberi, M. 2006. Tidal channel deposits on a  
763 delta plain from the upper Miocene Nauta Formation, Marañon foreland subbasin, Peru.  
764 *Sedimentology*, **53**, 971-1013, doi: 10.1111/j.1365-3091.2006.00795.x.

765 Reineck, H.E. & Wunderlich, F. 1968. Classification and origin of flaser and lenticular bedding.  
766 *Sedimentology*, **11**, 99-104.

767 Retallack, G.J. 2008. Soils of the past: an introduction to paleopedology. John Wiley & Sons.

768 Reynolds, A.D. 1999. Dimensions of paralic sandstone bodies. *AAPG Bulletin*, **83**, 211-229, doi:  
769 10.1306/00aa9a48-1730-11d7-8645000102c1865d.

770 Sisulak, C.F. & Dashtgard, S.E. 2012. Seasonal controls on the development and character of inclined  
771 heterolithic stratification in a tide-influenced, fluvially dominated channel; Fraser River, Canada.  
772 *Journal of Sedimentary Research*, **82**, 244-257, doi: 10.2110/jsr.2012.21.

773 Spalletti, L. 1995. Depósitos de tormenta en un frente deltaico. Jurásico medio de la Cuenca  
774 Neuquina, República Argentina. *Revista de la Sociedad Geologica de Espana*, **8**, 261-272.

775 Stukins, S., Jolley, D.W., McIlroy, D. & Hartley, A.J. 2013. Middle Jurassic vegetation dynamics from  
776 allochthonous palynological assemblages: An example from a marginal marine depositional setting;  
777 Lajas Formation, Neuquén Basin, Argentina. *Palaeogeography, Palaeoclimatology, Palaeoecology*,  
778 **392**, 117-127.

779 Taylor, A.M. & Goldring, R. 1993. Description and analysis of bioturbation and ichnofabric.  
780 *Geological Society of London, Journal*, **150**, 141-148.

781 Thomas, R.G., Smith, D.G., Wood, J.M., Visser, J., Calverley-Range, E.A. & Koster, E.H. 1987. Inclined  
782 heterolithic stratification; terminology, description, interpretation and significance. *Sedimentary*  
783 *Geology*, **53**, 123-179.

784 Uliana, M.A. & Legarreta, L. 1993. Hydrocarbons habitat in a Triassic-to-Cretaceous sub-Andean  
785 setting: Neuquen Basin, Argentina. *Journal of Petroleum Geology*, **16**, 397-420.

786 Urien, C.M. & Zambrano, J.J. 1994. Petroleum systems in the Neuquen Basin, Argentina. *In*: Magoon,  
787 L.B. & Dow, W.G. (eds.) *The petroleum system—from source to trap*, AAPG Memoir, 513-534.

788 Van Den Berg, J.H. 1987. Bedform migration and bed-load transport in some rivers and tidal  
789 environments. *Sedimentology*, **34**, 681-698, doi: 10.1111/j.1365-3091.1987.tb00794.x.

790 van den Berg, J.H., Boersma, J.R. & van Gelder, A. 2007. Diagnostic sedimentary structures of the  
791 fluvial-tidal transition zone; evidence from deposits of the Rhine and Meuse. *Geologie en Mijnbouw*.  
792 *Netherlands Journal of Geosciences*, **86**, 287-306.

793 van Maren, D.S. & Hoekstra, P. 2004. Seasonal variation of hydrodynamics and sediment dynamics in  
794 a shallow subtropical estuary: the Ba Lat River, Vietnam. *Estuarine, Coastal and Shelf Science*, **60**,  
795 529-540, doi: <http://dx.doi.org/10.1016/j.ecss.2004.02.011>.

796 Varela, A.N., Veiga, G.D. & Poire, D.G. 2012. Sequence stratigraphic analysis of Cenomanian  
797 greenhouse palaeosols: A case study from southern Patagonia, Argentina. *Sedimentary Geology*,  
798 **271-272**, 67-82, doi: 10.1016/j.sedgeo.2012.06.006.

799 Villard, P.V. & Church, M. 2003. Dunes and associated sand transport in a tidally influenced sand-bed  
800 channel: Fraser River, British Columbia. *Canadian Journal of Earth Sciences*, **40**, 115-130, doi:  
801 10.1139/e02-102.

802 Visser, M.J. 1980. Neap-spring cycles reflected in Holocene subtidal large-scale bedform deposits; a  
803 preliminary note. *Geology (Boulder)*, **8**, 543-546.

804 Willis, B.J. 2005. Deposits of tide-influenced river deltas. In: Bhattacharya, J.P. & Giosan, L. (eds.)  
805 *River Deltas—Concepts, Models, and Examples: SEPM, Special Publication*. Society for Sedimentary  
806 Geology (SEPM), Tulsa, OK, United States, 87-129.

807 Wilson, A., Flint, S., Payenberg, T., Tohver, E. & Lanci, L. 2014. Architectural styles and sedimentology  
808 of the fluvial lower Beaufort Group, Karoo Basin, South Africa. *Journal of Sedimentary Research*, **84**,  
809 326-348, doi: 10.2110/jsr.2014.28.

810 Zambrano, C.U.J. & Yrigoyen, M. 1995. Petroleum basins of southern South America: an overview. In:  
811 Tankard, A.J., Suárez, S.R. & J., W.H. (eds.) *Petroleum basins of South America*. Petroleum Basins of  
812 South America, 63-77.

813 Zavala, C. 1996a. High-resolution sequence stratigraphy in the Middle Jurassic Cuyo Group, South  
814 Neuquén Basin, Argentina. *GeoResearch Forum*, **1-2**, 295-303.

815 Zavala, C. 1996b. Sequence stratigraphy in continental to marine transitions; an example from the  
816 Middle Jurassic Cuyo Group, South Neuquén Basin, Argentina. *GeoResearch Forum*, **1-2**, 285-293.

817 Zavala, C. & González, R. 2001. Estratigrafía del Grupo Cuyo (Jurásico inferior-medio) en la Sierra de  
818 la Vaca Muerta, Cuenca Neuquina. *Boletín de Informaciones Petroleras*, **Tercera Época, año XVII**, 52-  
819 64.

820

## 821 **Figure captions**

822 **Fig. 1.** Pie chart highlighting the dominance of discharge fluctuations in modern rivers. Based  
823 on the database of Milliman and Farnsworth (2011).

824

825 **Fig. 2. (a)** Location map and extent of the Neuquén Basin. **(b)** Detailed location map showing  
826 the location of the study area (black rectangle).

827

828 **Fig. 3.** Middle Jurassic stratigraphy of the Neuquén Basin. Modified from Howell *et al.*  
829 (2005) and McIlroy *et al.* (2005). On the right, a detailed stratigraphic column of the Cuyo  
830 Group in the study area with a generalized palaeoenvironmental interpretation. The  
831 stratigraphic subdivisions on the left of the column are from Zavala (1996a, 1996b) and  
832 McIlroy *et al.* (2005).

833

834 **Fig. 4.** Representative photographs of the coarser- and finer-grained interbedding in major  
835 and minor channel deposits in the Lajas Fm. interpreted as river flood and interflood beds  
836 formed in response to fluctuations in river discharge. Photos are from the upper part of the  
837 stratigraphy. **(a)** Distributary channels deposits (FA 1) overlying floodplain deposits (FA 2).

838 The channel deposits show a structureless part and a low-angle interbedded part with coarser-  
839 (river flood) and finer-grained (interflood) deposits. Dashed lines indicate erosional surfaces  
840 at the base of the unit. Triangles indicate fining- and thinning-upward trends. Person for scale  
841 is 1.75 m tall. **(b-c)** Detail of distributary channel deposits (FA 1) with alternation of coarser-  
842 (river flood) and finer-grained (interflood) beds. Finer-grained beds are marked by abundant  
843 carbonaceous material **(b)** and trace fossils **(c)** indicating lower energy. Compass for scale is  
844 6.5 cm long and pencil for scale is 12 cm long. **(d)** Minor distributary channel deposits (FA  
845 3) showing alternations of coarser- (river flood) and finer-grained (interflood) beds. Dashed  
846 lines indicate erosional surfaces at the base of the unit. Triangles indicate fining- and  
847 thinning-upward trends. **(e)** Detail of minor distributary channel deposits (FA 3) with  
848 alternation of coarser- (river flood) and finer-grained (interflood) beds. Syneresis cracks in  
849 the interflood bed mark a salinity contrast. Pencil for scale is 12 cm long.

850

851 **Fig. 5. (a-b)** Cyclical pattern in carbonaceous drapes in unidirectional, seaward-oriented  
852 cross-stratification interpreted as the result of tidal modulation of fluvial currents. Arrows  
853 show tidal modulation cycles indicated by spacing of the drapes or the height reached by  
854 drapes in the dune foresets. Grain size card for scale in **(a)** is 8 cm long. Note 10 cm scale bar  
855 in **(b)**.

856

857 **Fig. 6. (a-c)** Representative photographs of the coarser- and finer-grained interbedding in  
858 crevasse mouth bars (FA 4) of the Lajas Fm., interpreted as river flood and interflood beds  
859 formed as a result of river discharge fluctuations. Photos are from the upper part of the  
860 stratigraphy. The triangle indicates coarsening- and thickening-upward trend. Notebook for  
861 scale is approximately 20 cm long and lens cap is 52 mm in diameter. See key for the  
862 sedimentary log in Fig. 4.

863

864 **Fig. 7.** Representative photographs of the coarser- and finer-grained interbedding in mouth  
865 bars (FA 6) of the Lajas Fm., interpreted as river flood and interflood beds formed as a result  
866 of river discharge fluctuations. Photos are from the lowest 200 m of the stratigraphy. **(a)** Two  
867 stacked mouth bar units with the associated sedimentary log. Person for scale is 1.75 m tall.  
868 Triangles indicate coarsening- and thickening-upward trends. See key for the sedimentary log  
869 in Fig. 4. **(b)** Amalgamated river flood beds in the upper part of the FA 6 unit. **(c)** River flood  
870 and interflood beds in the medial part of the unit. **(d-e)** Interbedding formed by fluvial  
871 discharge fluctuations from the lower 100 m of the stratigraphy. Note that interflood beds are  
872 highly bioturbated (BI 6) compared to unbioturbated river flood beds. Pencil for scale is  
873 about 12 cm long and coin is about 2.5 cm in diameter.

874

875 **Fig. 8.** Summary of the key characteristics of river flood and interflood beds from mouth-bar  
876 deposits (FA 6). Pen for scale is 12 cm long.

877

878 **Fig. 9.** Formation of bedding in a mouth-bar setting in response to seasonal discharge  
879 variations with a weak tidal overprint during the interflood period. Length of arrow represents  
880 strength/velocity of fluvial and tidal currents.

881

882 **Fig. 10.** Schematic depositional model for the studied sections of the Lajas Fm. showing the  
883 distribution of facies with and without seasonal bedding.

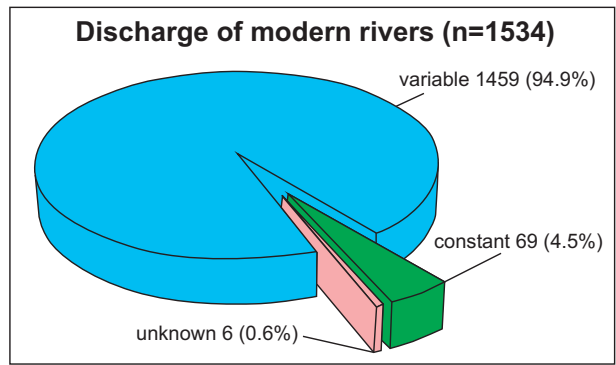


**Figure 1**

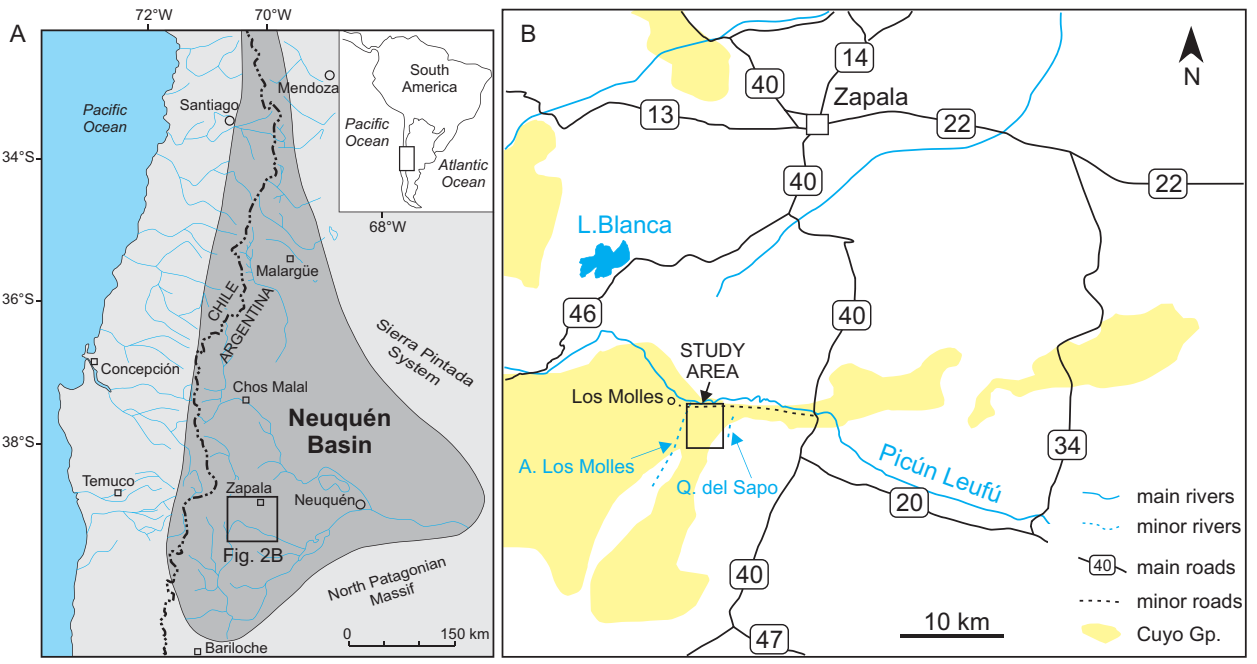


Figure 2

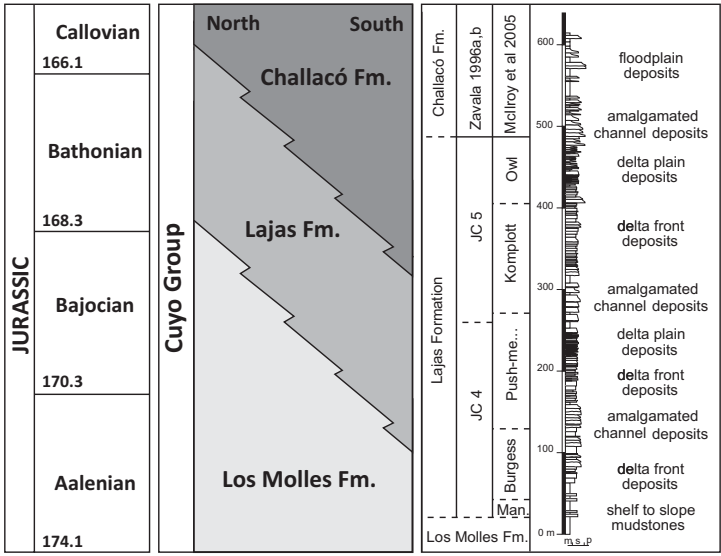


Figure 3

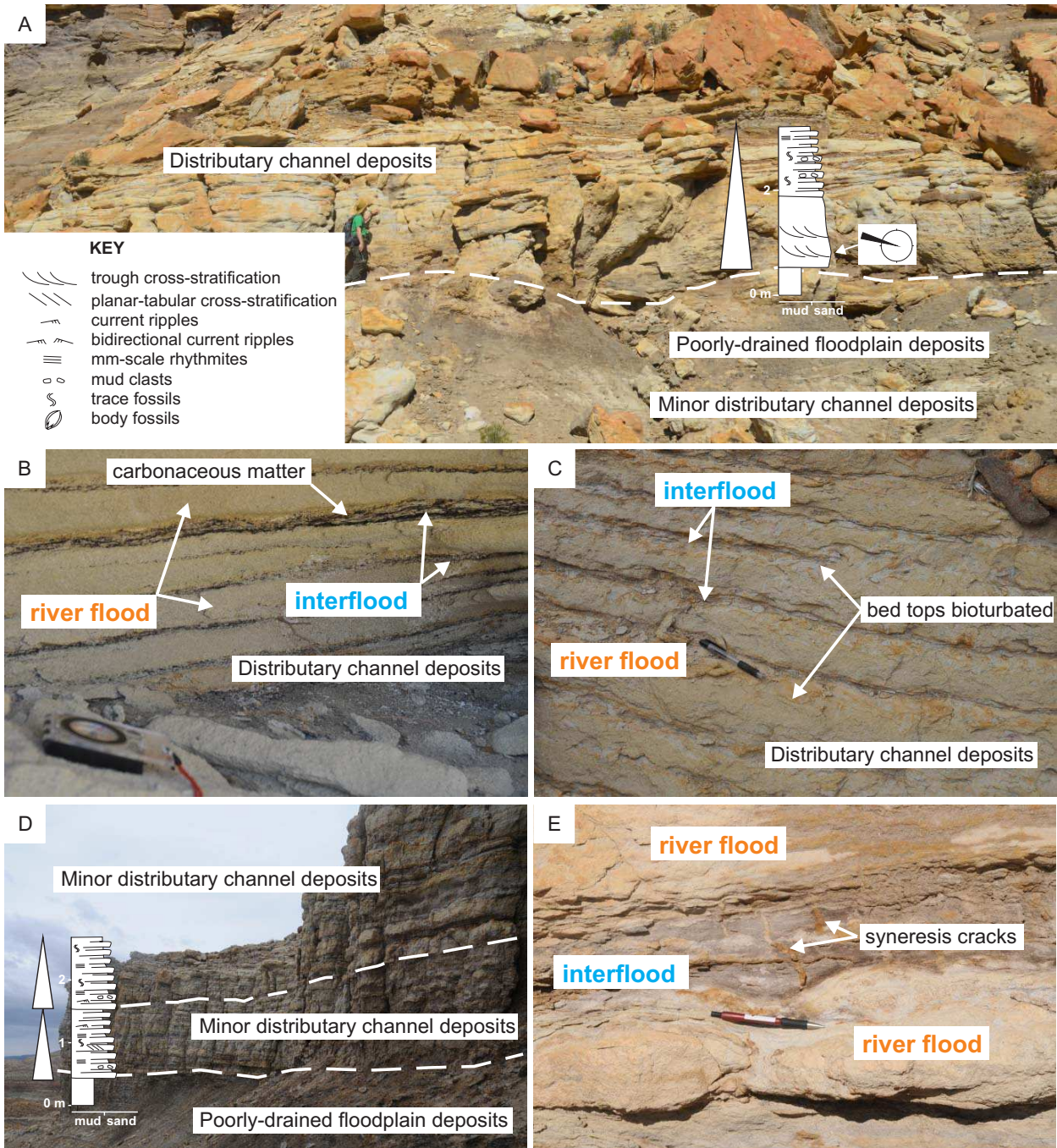


Figure 4

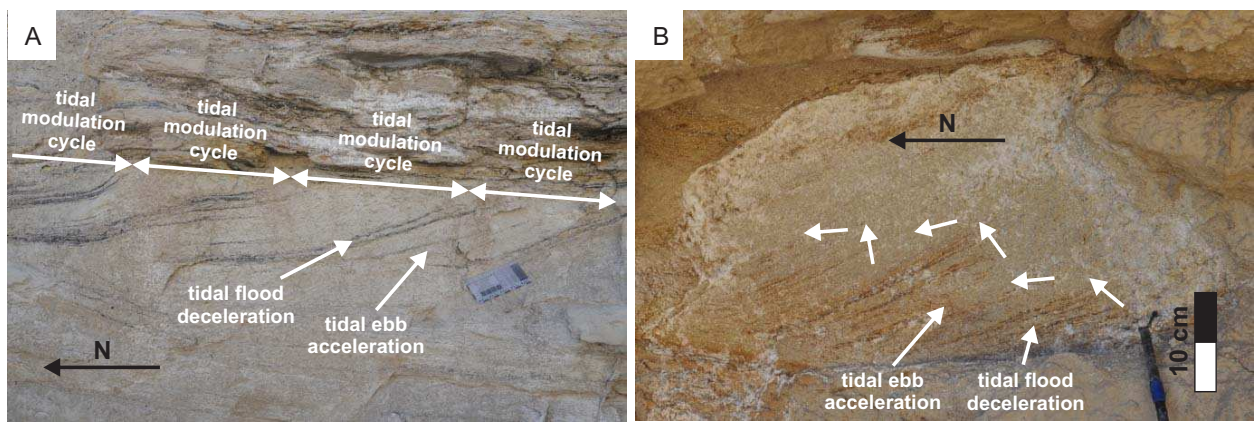


Figure 5

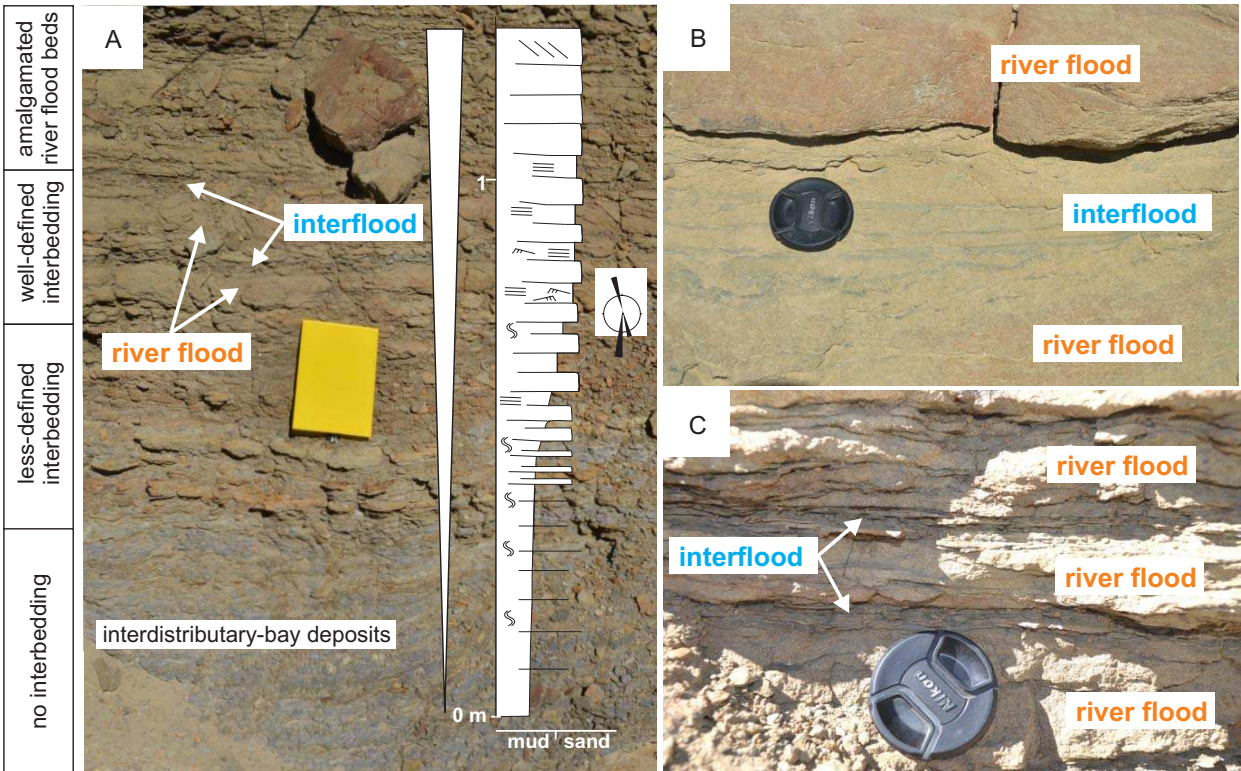


Figure 6

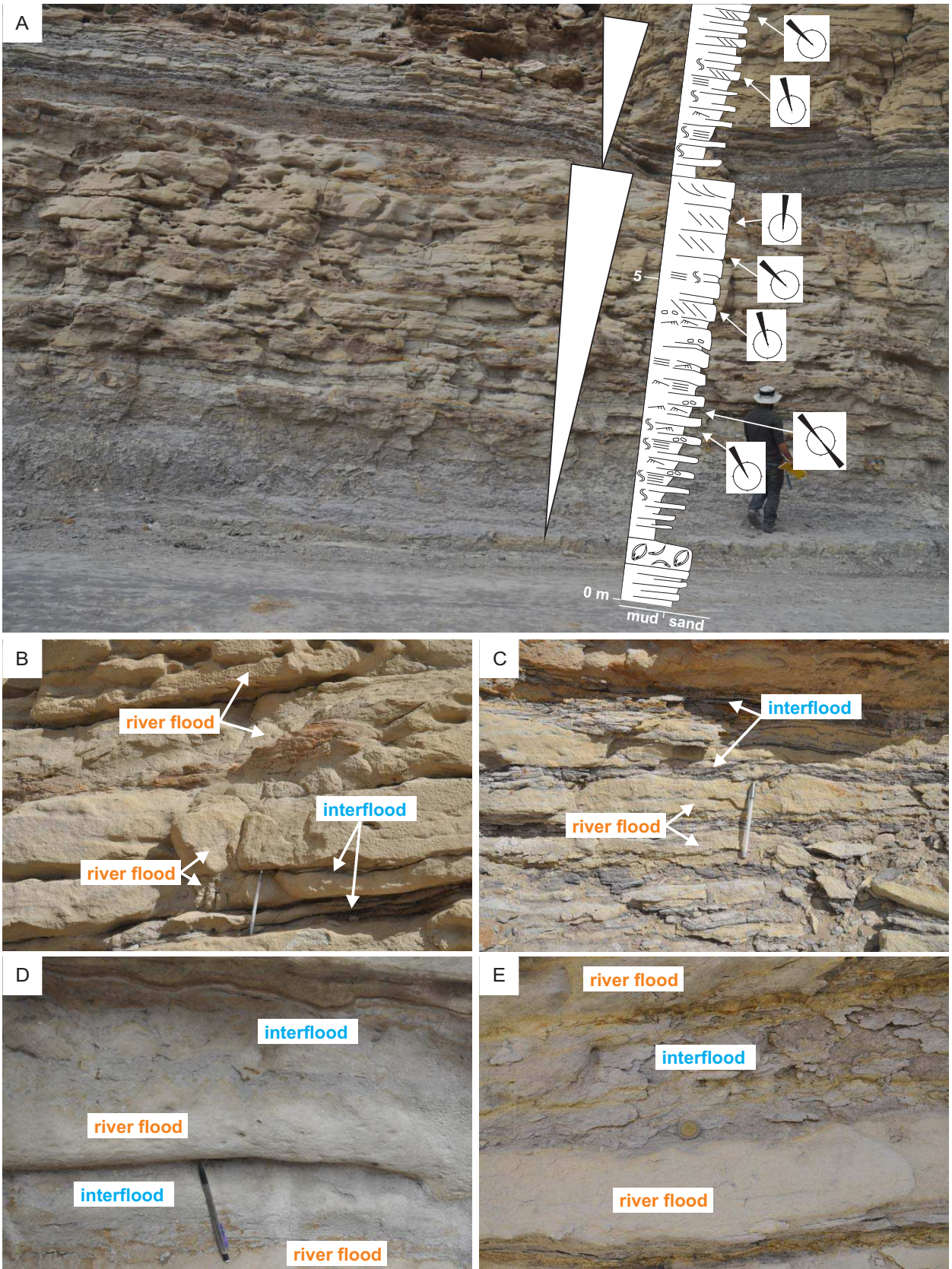


Figure 7

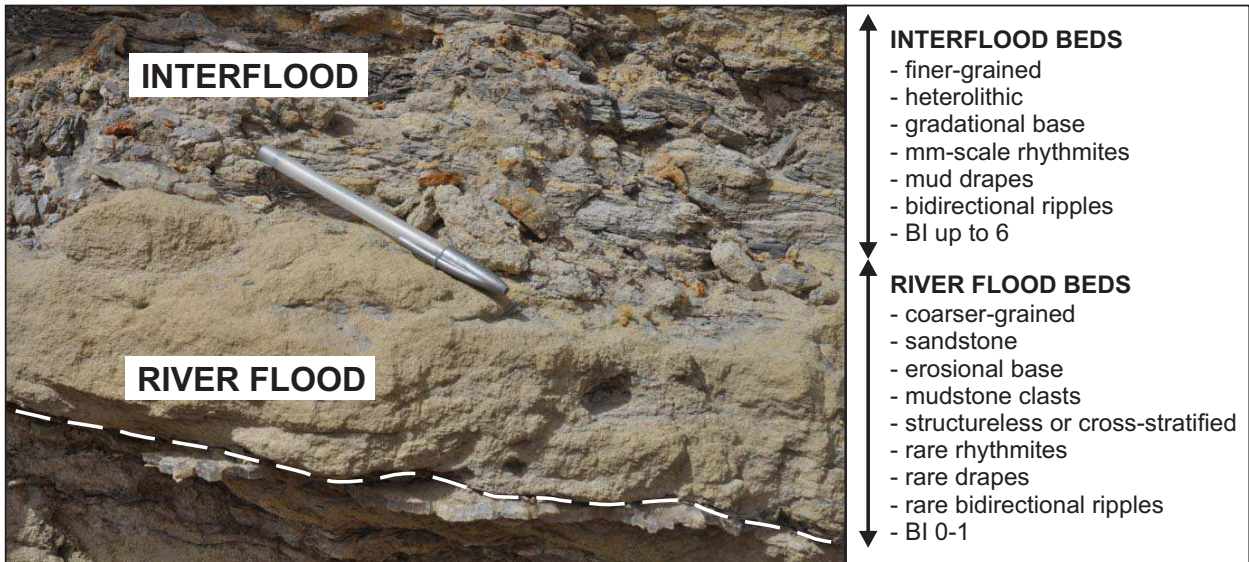


Figure 8

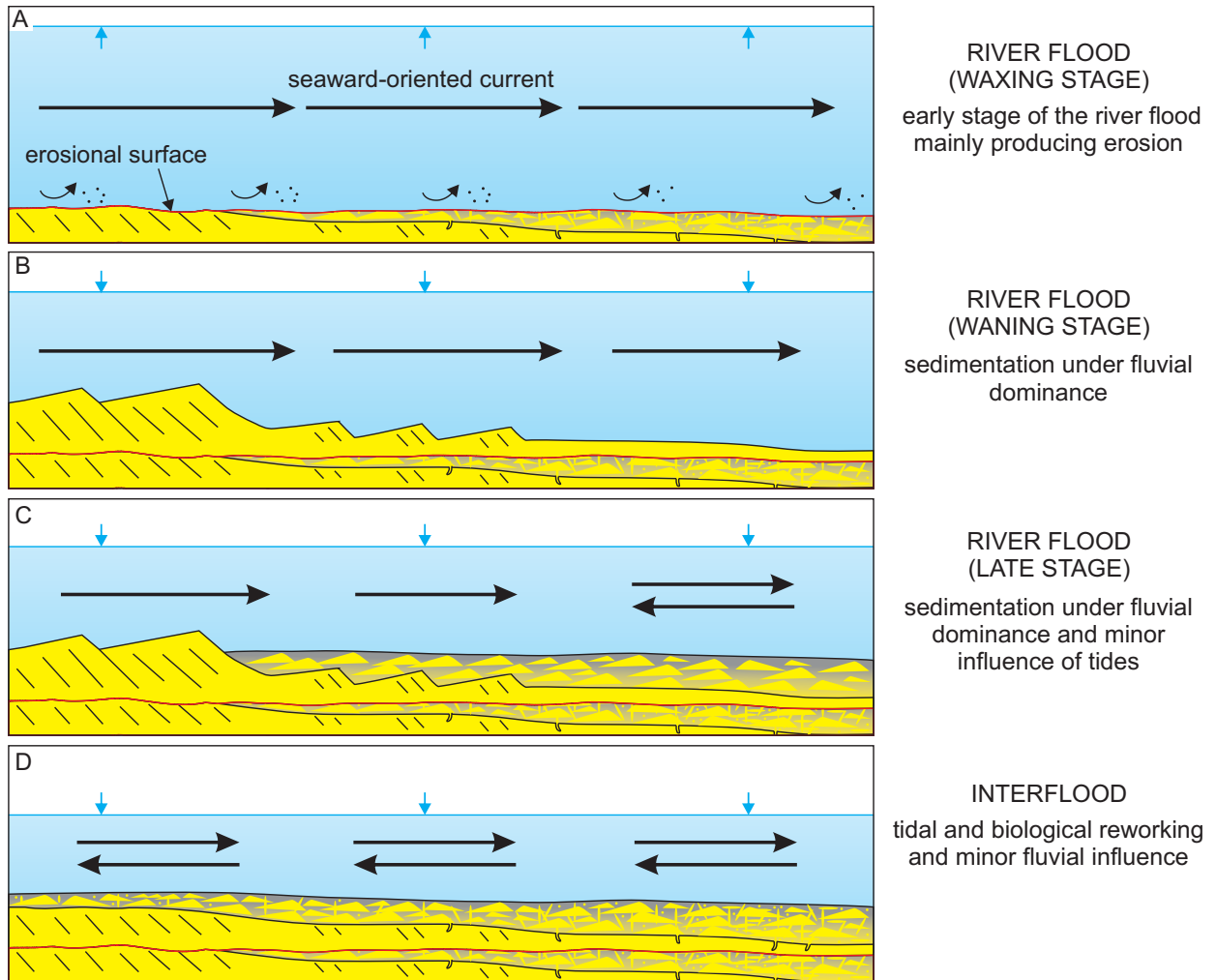


Figure 9

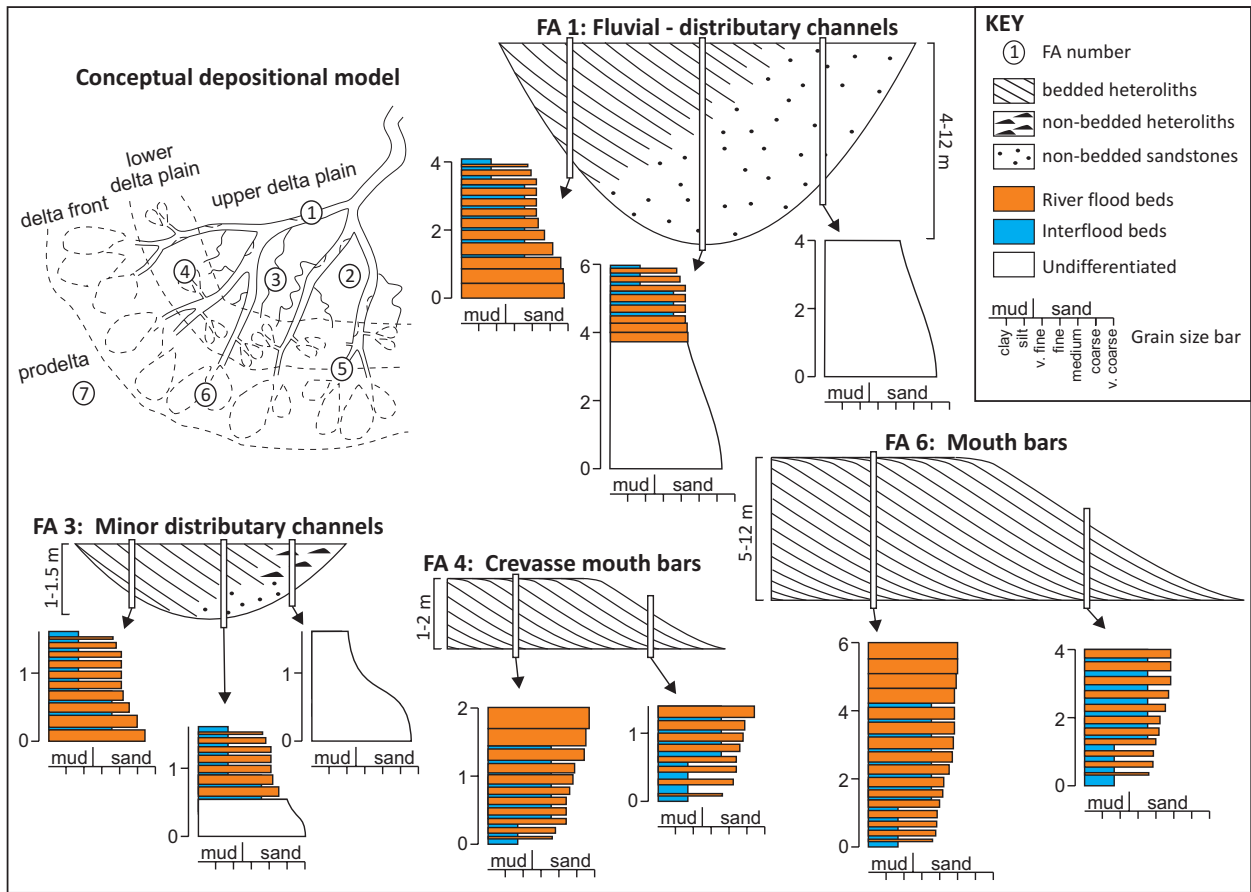


Figure 10